

Development of a MEMS Device for Acoustic Emission Testing

Didem Ozevin^a, Stephen Pessiki^a, Akash Jain^b, David W. Greve^b, Irving J. Oppenheim^{c*}

^aDept. of Civil and Environmental Engineering, Lehigh University, Bethlehem, PA 18015

^bDept. of Electrical and Computer Engineering, Carnegie Mellon University, Pittsburgh, PA 15213

^bDept. of Civil and Environmental Engineering, Carnegie Mellon University, Pittsburgh, PA 15213

ABSTRACT

Acoustic emission testing is an important technology for evaluating structural materials, and especially for detecting damage in structural members. Significant new capabilities may be gained by developing MEMS transducers for acoustic emission testing, including permanent bonding or embedment for superior coupling, greater density of transducer placement, and a bundle of transducers on each device tuned to different frequencies. Additional advantages include capabilities for maintenance of signal histories and coordination between multiple transducers. We designed a MEMS device for acoustic emission testing that features two different mechanical types, a hexagonal plate design and a spring-mass design, with multiple detectors of each type at ten different frequencies in the range of 100 kHz to 1 MHz. The devices were fabricated in the multi-user polysilicon surface micromachining (MUMPs) process and we have conducted electrical characterization experiments and initial experiments on acoustic emission detection. We first report on C(V) measurements and perform a comparison between predicted (design) and measured response. We next report on admittance measurements conducted at pressures varying from vacuum to atmospheric, identifying the resonant frequencies and again providing a comparison with predicted performance. We then describe initial calibration experiments that compare the performance of the detectors to other acoustic emission transducers, and we discuss the overall performance of the device as a sensor suite, as contrasted to the single-channel performance of most commercial transducers.

Keywords: Acoustic emission, MEMS, plate, diaphragm, spring-mass, capacitive sensing, characterization, sensitivity

1. INTRODUCTION

Acoustic emissions are transient stress waves generated by the rapid release of energy from localized sources within a material. Acoustic emission testing is a method to evaluate the behavior of structural materials, and in particular to identify the onset of damage, through the detection and evaluation of these transient stress waves. The released energy propagates through the object as stress waves, and the arrival of the stress waves are detected by an acoustic emission transducer coupled to the surface of the object. This transducer converts the mechanical disturbance at the surface of the object into an electrical signal.

Piezoelectricity is the transduction principle used in most acoustic emission transducers. Transducers designed specifically for acoustic emission testing are similar to acceleration transducers except that they do not need a proof mass, but rather a special backing and coupling layer¹. Research has been performed to improve the capabilities of acoustic emission transducers since the 1980s. Proctor² developed a broadband piezoelectric transducer, which consists of a conical active element and an extended backing. Small transducer contact area, elimination of acoustical interference effects associated with certain geometries and redistribution of arrival times of reflected signals originating from various elements of the transducer were the guiding criteria in the design. But, the overall size of the transducer makes it inconvenient for small specimen testing and on-site application. Lee and Kuo³ reduced the aperture size of the piezoelectric element to 200 μm in diameter using the micro-fabrication capability of an excimer laser. Evans et al.⁴ showed the applicability of conical piezoelectric transducers as point acoustic sources. Although most work to date has used piezoelectric ceramic sensors, some alternate approaches have been explored. Or et al.⁵ reported that

* Contact author: ijo@cmu.edu; 412-268-2950; Carnegie Mellon University, Department of Civil and Environmental Engineering, Pittsburgh, PA 15213.

polyvinylidene fluoride/trifluoroethylene (P(VDF-TrFE)) copolymer was superior to piezoelectric ceramic. Marm-Franch et al.⁶ tested PTCa/PEKK piezo-composites for surface mounting and embedding. Breckenridge and Greenspan⁷ used a capacitive transducer for surface displacement measurement.

2. PREVIOUS WORK

The application of MEMS technology to acoustic emission testing is a new research area. However, there are several reports on the application of MEMS to the related problem of ultrasonic testing. Khuri-Yakub et al.^{8, 9} presented a capacitive MEMS ultrasonic transducer (cMUT) which could replace piezoelectric transducers, and demonstrated air-coupled and immersion applications. Several innovative processes in the device fabrication to optimize transducer performance were reported¹⁰. Bashford et al.¹¹ also showed the superiority of water-coupled micromachined ultrasonic capacitance transducers to piezoelectric transducers. Greve et al.^{12, 13} studied solid coupled and phased array applications of capacitive diaphragm transducers fabricated using the MUMPS process. To sense mechanical vibration at frequencies of interest for wear state recognition, below 10 kHz, Scheibner et al.¹⁴ reported the development of a frequency selective micromachined array for vibration measurement; the array was constructed in a single-crystal silicon process and was tunable through stress-stiffening and through electrostatic softening.

3. TECHNICAL APPROACH

Acoustic emission sources are complex transient signals produced by broadband energy sources. Acoustic emission transducers should preferably cover a wide frequency spectrum in order to localize and identify the sources. The frequency range of interest in acoustic emission measurements of metals and brittle materials is from 100 kHz to 1 MHz¹⁵. Whereas broadband sensors are commonly used, we hypothesize that a suite of many narrowband sensors covering the frequency range of interest would demonstrate superior sensing. We have designed capacitive-type MEMS transducers, to respond to displacements normal to their plane, using the following criteria:

- simple design to minimize stray capacitances,
- minimum gap between the stationary plate and the movable plate, and maximum number of units in parallel in each detector to enhance the sensitivity,
- several resonant transducers on one chip to span the frequency range of interest.

4. DEVICE DESIGN

Our capacitive type transducers feature a capacitor with one stationary plate and one plate free to move. The two plates are separated by air gap. The quantity to be measured by the transducers is the normal surface displacement of the solid on which the chip is mounted. The devices were fabricated in the MUMPs process. There are two mechanical configurations on the chip, referred to as the hexagonal plate design and the piston design. A total of 18 independent transducers are placed on a 1cm² chip as shown in Figure 1.

4.1 Hexagonal plate design

The first configuration is similar to the ultrasonic design of Greve et al.¹², but with longer edge lengths in order to be resonant at lower frequencies. The DIMPLE mask in the MUMPS process was employed, reducing the gap between the electrodes to 1.25 μm and thereby increasing the capacitance of each detector. The change in capacitance is created by a change in the gap dimension as a result of diaphragm deflection. Hexagonal diaphragms were designed at five different frequencies between 300 kHz and 1 MHz; two transducers at each of the three lowest frequencies and one transducer at each of the two highest frequencies were fabricated on the chip. Figure 2 shows a single detector unit and its SEM picture. Within each transducer between 36 and 105 hexagonal units are connected in parallel to increase the sensitivity.

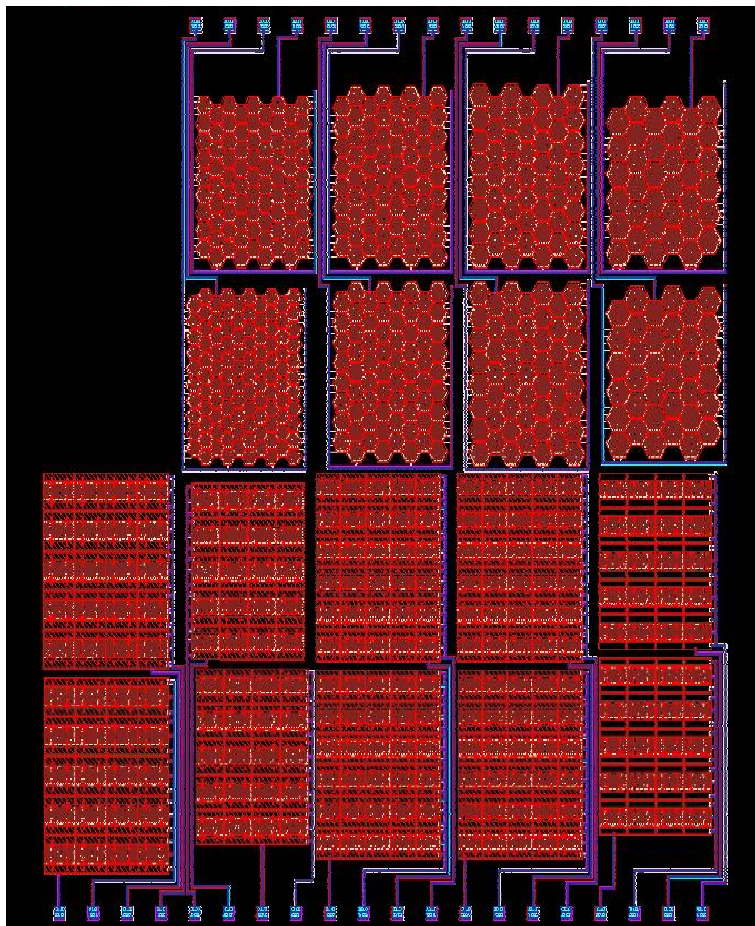
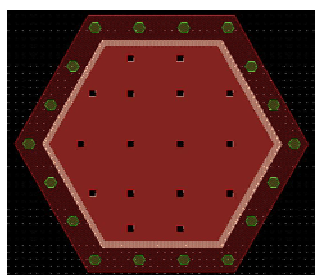
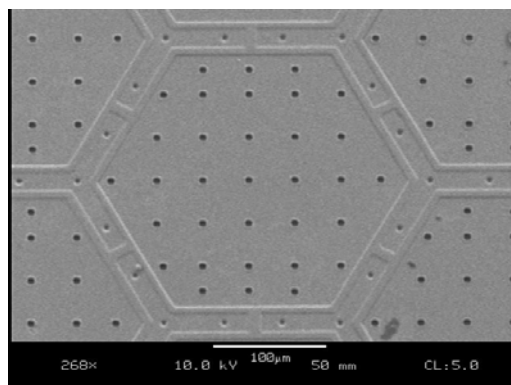


Figure 1. Chip layout



(a)



(b)

Figure 2. (a) A single hexagonal type transducer detector unit, (b) SEM view

4.2 Spring-mass (piston) design

The second configuration is referred to as a spring-mass design or a piston design, where the change in capacitance results from an out-of-plane rigid body motion. Piston designs were constructed at five different frequencies ranging from 100 kHz to 300 kHz, achieved by varying the edge length of the mass unit and by varying the dimensions of the spring elements. Figure 3 shows a detector group and its SEM picture. Depending upon the size, either 20 or 30 pistons are connected in parallel to increase the sensitivity of each transducer. Conducting links, Z-shaped in plan, achieve electrical connectivity of these groups, but the pistons are not continuously connected mechanically in order to prevent adverse effects of residual stress.

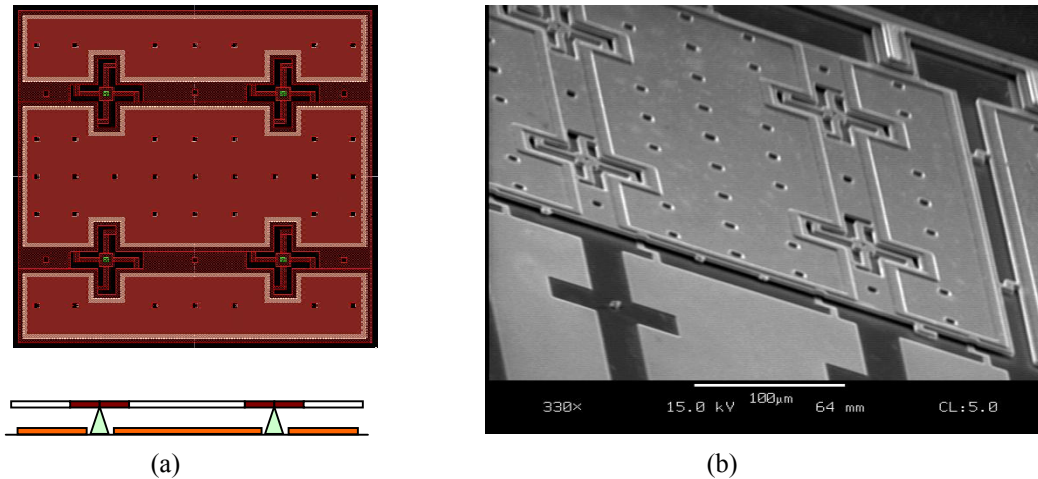


Figure 3. (a) A single piston type transducer detector unit, (b) SEM view

5. CHARACTERIZATION OF DEVICE PROPERTIES

The devices were delivered as post-processed chips, with release etching and supercritical drying completed. The backsurfaces were metallized and then the chips were mounted in ceramic packages with silver epoxy. The contact pads were then connected to the package pins by wirebonding.

5.1 C-V measurements

When a DC voltage is placed between two electrodes of a capacitor, the Coulomb force produces an attraction between the plates, and the diaphragm will deflect accordingly. The electrostatic Coulomb force, applied to an elastic diaphragm structure, results in a parabolic relationship between capacitance and voltage in the form $C(V) = C_0 + C_1V^2$, where C_0 is the capacitance of the undeflected device. C-V measurements of devices were performed and the experimental results were compared with the predictions as shown in Table 1 and Table 2 for hexagonal designs and piston designs, respectively. Comparing the experimental results and the predictions, the main reason for the difference in C_0 is the stray capacitance, even though the stray capacitances had been minimized as much as possible. The results show that both configurations yield operating transducers with resonant frequencies near their design values. Figure 4 shows typical C-V plots for hexagonal and piston type designs.

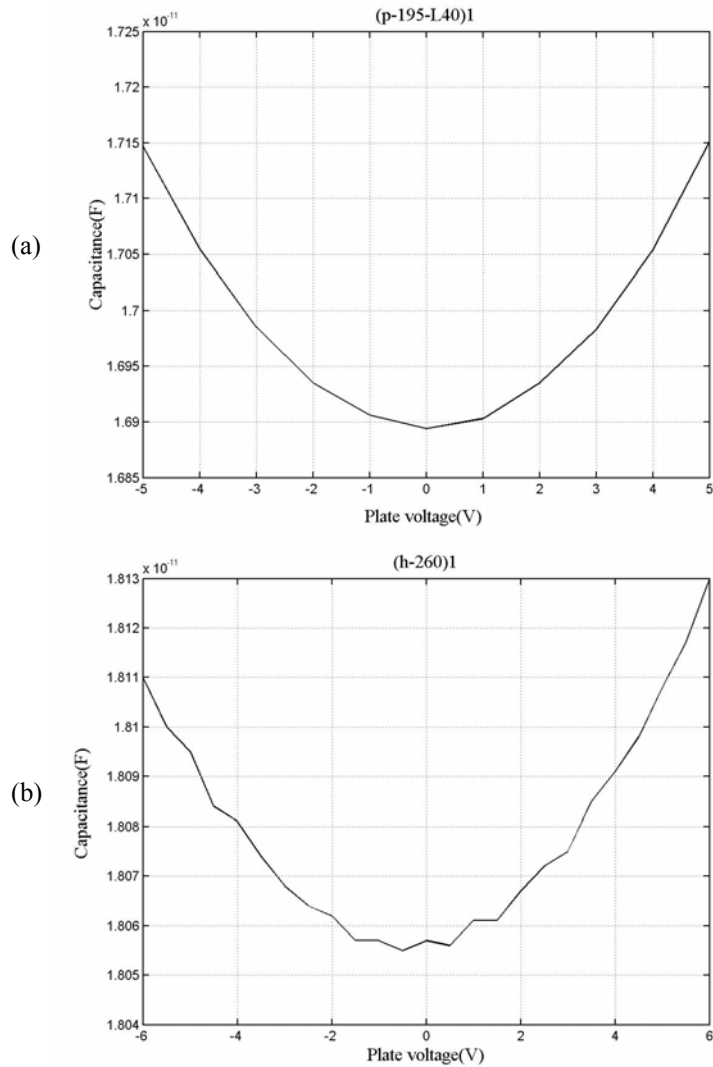


Figure 4. C-V plots of (a) a piston type device, (b) a hexagon type device

5.2 Admittance (resonance) measurements

In admittance tests, the response of devices to the flow of a small AC voltage at a given frequency is measured. In the presence of a DC bias voltage, the equivalent circuit model¹² shows that there is a sharp change in admittance and phase values at the resonant frequency of the device. This is in effect a forced vibration of the device, and such tests verify the resonant frequencies of the devices. Figure 5 shows typical admittance measurements for hexagon and piston type designs. In each case the tests were performed with an applied DC bias voltage (either 5 or 6 V) and also in the absence of a DC bias voltage; as expected, in the absence of a DC bias voltage there is no mechanical resonance effect. The admittance tests were performed under both atmospheric pressure and under vacuum. The transducers are somewhat damped under atmospheric pressure because of a squeeze-film effect as air passes through the etch holes on the devices; consequently, the packages were sealed and evacuated to create a vacuum environment, creating high Q transducers and making it easy to identify resonant frequencies.

Table 1 shows the results of admittance measurements on the hexagonal plate design and their comparison with predictions. The diaphragms were modeled as circular plates, with the same area as the hexagonal plates. The modal

frequencies for simple support and fixed support assumptions were computed by an analytical formula¹⁶, using material properties of 160 GPa for Young’s modulus and 0.3 for Poisson’s ratio. As seen in Table 1, the measured resonant frequencies lie between the frequencies predicted for simple and fixed support conditions, but closer to the fixed support case.

For piston type designs, anchors were modeled as fixed supports because spring elements are located symmetrically at each anchor. In addition, the connections between the spring structures and the mass were considered as rotationally rigid within the plane of the piston. Two resonances are observed within the range of admittance measurement as seen in Figure 5a, presumably corresponding to out-of-plane rotation and translation. While the predicted resonant frequencies are lower than the experiment results for two designs (p_195_L40) and (p_175_L40) of relatively low design frequency, the predicted resonant frequencies become higher than the experimental results for stiffer designs. In-plane residual stresses, design assumptions, and uncertainties in the micromachining process might be reasons for the differences between predicted and experimental results.

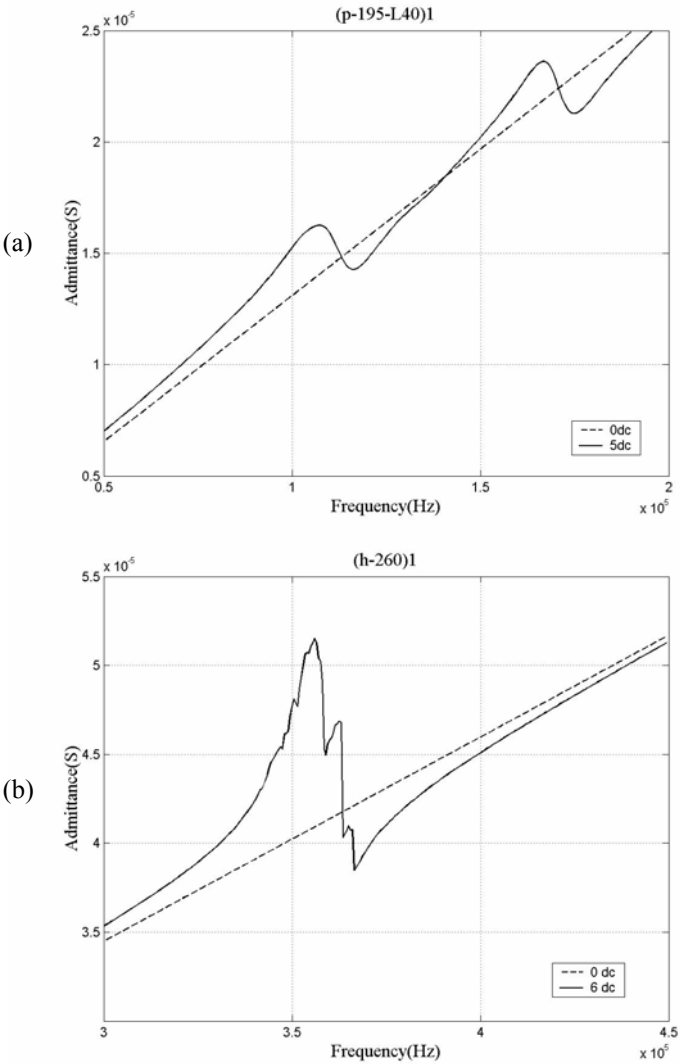


Figure 5. Impedance plots of (a) a piston type device, (b) a hexagon type device

Table 1. Comparison of characterization measurements with predictions, hexagonal type design

Device*	C0(F)		C1(F)		f(kHz)		
	Experiment	Simple support Prediction	Experiment	Simple support Prediction	Experiment	Simple support Prediction	Fixed support Prediction
(h_155)1*	1.68E-11	1.18E-11	5.33E-16	3.55E-16	1065	595	1220
(h_175)1	1.63E-11	1.30E-11	7.28E-16	6.32E-16	812	467	958
(h_195)1	1.73E-11	1.38E-11	1.38E-15	1.02E-15	658	376	771
(h_195)2	3.02E-11	1.38E-11	1.63E-15	1.02E-15	662	376	771
(h_225)1	1.90E-11	1.46E-11	3.04E-15	1.89E-15	482	282	579
(h_225)2	1.92E-11	1.46E-11	4.28E-15	1.89E-15	483	282	579
(h_260)1	1.99E-11	1.35E-11	4.93E-15	3.07E-15	359	211	434
(h_260)2	1.95E-11	1.35E-11	4.88E-15	3.07E-15	366	211	434

* (h_xxx)y: hexagonal design, which has xxx edge length and y number of its copies.

Table 2. Comparison of characterization measurements with predictions, piston type design

Device*	C0(F)		C1(F)		F(kHz)			
	Experiment	Prediction	Experiment	Prediction	Experiment		Prediction	
					Mode1	Mode2	Rotational	Translational
(p_195_L40)1	1.99E-11	1.60E-11	1.53E-14	1.21E-14	112	166	97	112
(p_195_L40)2	1.78E-11	1.60E-11	1.14E-14	1.21E-14	112	164	97	112
(p_175_L40)1	1.61E-11	1.06E-11	8.43E-15	6.14E-15	131	206	108	126
(p_175_L40)2	1.64E-11	1.06E-11	7.24E-15	6.14E-15	136	197	108	126
(p_175_L30)1	1.56E-11	1.26E-11	4.88E-15	3.17E-15	152	225	166	192
(p_175_L30)2	1.59E-11	1.26E-11	4.77E-15	3.17E-15	153	224	166	192
(p_155_L26)1	1.71E-11	1.42E-11	2.92E-15	1.72E-15	194	293	232	270
(p_155_L26)2	1.71E-11	1.42E-11	3.01E-15	1.72E-15	196	294	232	270
(p_155_L20)1	1.73E-11	1.44E-11	2.09E-15	8.19E-16	211	326	343	394
(p_155_L20)2	1.78E-11	1.44E-11	2.22E-15	8.19E-16	211	324	343	394

* (p_xxx_Lyy)z: piston design, which has xxx unit-mass edge, yy spring element length and z number of its copies.

6. EXPERIMENTAL RESULTS AT SIGNAL DETECTION

In order to characterize the mechanical behavior of MEMS transducers, a steel test specimen as shown in Figure 6 was constructed. This design provides for a path length of 2.54 cm between a MEMS transducer under investigation and an ultrasonic or acoustic emission source located on the opposing surface. Three experiments were performed to estimate the sensitivity of the MEMS transducers: (a) the MEMS transducers were excited by a commercial ultrasonic transducer, (b) a commercial ultrasonic transducer was excited by a commercial ultrasonic transducer, and (c) a commercial ultrasonic transducer was excited by a pencil break to simulate an acoustic emission burst. Conditions that would minimize the coupling of externally generated noise, such as careful shielding and low-noise preamplification, were not employed in these pilot experiments.

In the first and second experiments, a Krautkramer 1-MHz MSW-QC ultrasonic transducer was used as the excitation source, driven by a Krautkramer USPC-2100 operated at 75-ohm pulser damping with HI pulser voltage and HI pulser energy settings. In the first experiment the MEMS transducers were made as sensitive as reasonably possible by operating in vacuum at a relatively large DC bias voltage, with an amplifier having a gain of 50 together with 300 Hz high pass and 1 MHz low pass filtering. Figures 7a and 9a show the excitation signal from the ultrasonic transducer. The amplitude of the exciting pulse, at 19.8 μ s, is clipped due to amplifier saturation, and reflections are detected at subsequent 9 μ s intervals. As expected, the MEMS transducers received the signal at approximately 25 μ s as seen in Figure 7b and Figure 9b. The amplitudes of the received signals (with the amplifier gain of 50, averaged 256 times) for the hexagonal and piston designs are about 40 mV and 10 mV, respectively, as shown in Table 3. Note the ringing of the transducer in both cases. The experiment also verifies the resonant frequencies obtained by admittance measurements. Figures 8 and Figure 10 show FFT plots of the signals detected by the hexagonal and piston type designs, respectively. The MEMS transducers have a very narrow bandwidth at their resonant frequencies and show a zero frequency response below resonance. Figure 7c and Figure 9c represent control tests at zero bias voltage.

In the second experiment, a commercial ultrasonic transducer was used as the receiver in place of the MEMS device, as shown in Figure 6b. The amplitude of the received signal was found to be 2.3 V, shown in Table 3. This result suggests that as a receiver the Krautkramer 1-MHz MSW-QC ultrasonic transducer is more sensitive by a factor of about 57 ($=2.3V/40mV$) than the hexagonal design after amplification.

In the third experiment, keeping the commercial ultrasonic transducer as the receiver, a pencil break was used as the excitation, yielding a one-shot received signal of 90 mV, as shown in Table 3. By proportion, the expected signal amplitude for MEMS transducers excited by a pencil break is predicted to be 1.56 mV and 0.39 mV for hexagonal and piston designs, respectively, as shown in Table 3. These signal amplitudes are within the range of the noise in the current MEMS implementation, roughly 2 mV, making it impractical to trigger on a one-shot signal of that amplitude. A low-noise amplifier is being developed and pencil break experiments with MEMS transducers will follow.

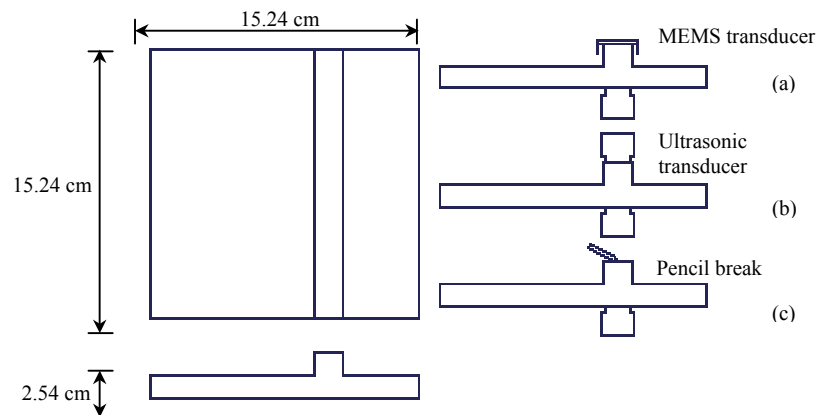


Figure 6. Schematic diagram of experimental arrangement, (a) MEMS transducer as receiver and ultrasonic transducer as excitation, (b) ultrasonic transducer as both receiver and excitation, (c) ultrasonic transducer as receiver and pencil break as excitation

Table 3. Experimental results

Excitation	Signal Amplitude (V)		
	Detector		
	Ultrasonic transducer	MEMS transducer	
Hexagonal design		Piston design	
Ultrasonic transducer	2.3	0.04	0.01
Pencil break	0.09	0.00156 (predicted)	0.00039 (predicted)

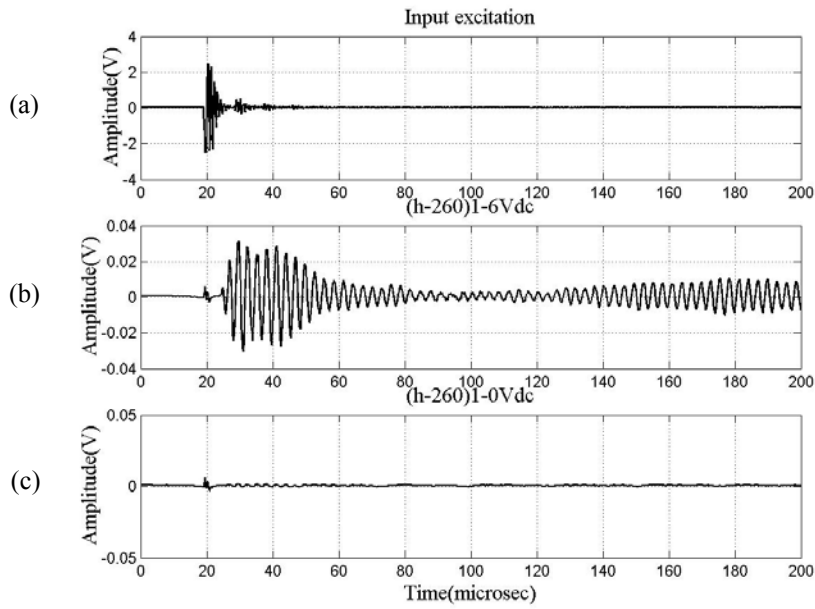


Figure 7. Ultrasonic experiment result, (h-260)1 (a) Excitation signal, (b) Received signal at $V_{DC}=6V$, (c) at $V_{DC}=0V$

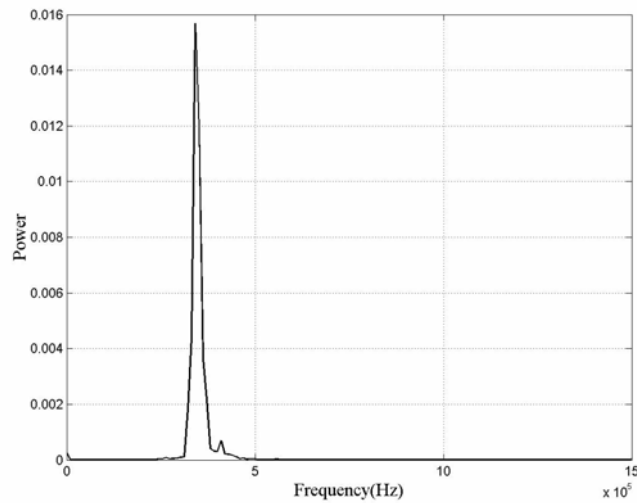


Figure 8. FFT of (h-260)1

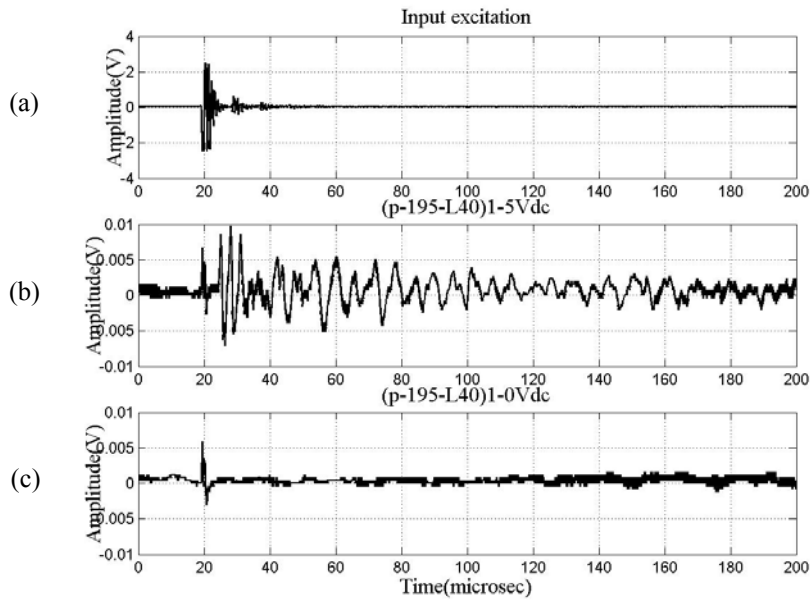


Figure 9. Ultrasonic experiment result, (p-195-L40)1, (a) Excitation signal, (b) Received signal at $V_{DC}=5V$, (c) at $V_{DC}=0$

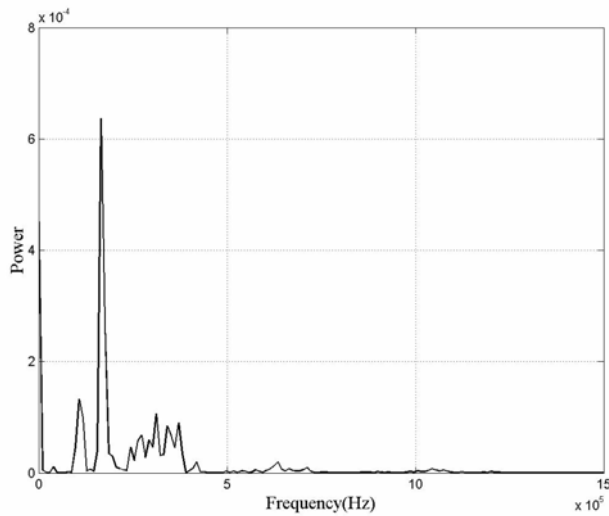


Figure 10. FFT of (p-195-L40)1

7. CONCLUSIONS

MEMS transducers for acoustic emission testing, which are sensitive to normal surface displacement, have been developed. A group of 18 independent capacitive type MEMS transducers were placed on a 1cm^2 chip and fabricated in the MUMPS process. The resonant frequencies of the transducers ranged from 100 kHz to 1 MHz, covering the frequencies of interest for acoustic emission testing. Electrical and initial mechanical characterization tests show that all configurations fulfill their operational requirements. Experiments with standard acoustic emission simulations, such as pencil break excitations, and the application of multi-channel experiments are underway.

One important potential contribution of a MEMS device would be the ability to detect a signal at different frequencies in one experiment. In addition, a surface micromachined MEMS device could be manufactured together with electrical circuits, making an integrated amplifier and embedded application possible. An embedded chip would eliminate the coupling problem encountered when temporarily mounting conventional transducers and would permit continuous monitoring; an integrated amplifier would contribute improved sensitivity.

ACKNOWLEDGEMENTS

This research was funded by a grant from the Pennsylvania Department of Community and Economic Development through the Pennsylvania Infrastructure Technology Alliance and by the Office of Naval Research, with equipment support from Krautkramer. Additional support was provided by the Center for Advanced Technology for Large Structural Systems at Lehigh University, and by the Institute for Complex Engineered Systems at Carnegie Mellon University. The authors gratefully acknowledge these sources of support.

REFERENCES

1. Gautschi, G., *Piezoelectric Sensorics*, Springer, 2002.
2. Proctor, T.M., "An Improved Piezoelectric Acoustic Emission Transducer," *Journal of Acoustic Society of America*, Vol.71, May 1982, pp.1163-1168.
3. Lee, Y.C., S.H. Kuo, "Miniature Conical Transducer Realized by Excimer Laser Micro-machining Technique," *Sensors and Actuators*, Vol.93, No.1, Aug. 2001, pp.57-62.
4. Evans, M.J., J.R. Webster, P. Cawley, "Design of a Self-calibrating Simulated Acoustic Emission Source," *Ultrasonics*, Vol.37, No.8, Jan. 2000, pp.589-594.
5. Or, S.W., H.L.W. Chan, C.L. Choy, "P(VDF-TrFE) Copolymer Acoustic Emission Sensors," *Sensors and Actuators*, Vol.80, No.3, Mar. 2000, pp.237-241.
6. Marm-Franch, P., T. Martin, D.L. Tunnicliffe, D.K. Das-Gupta, "PTCa/PEKK Piezo-composites for Acoustic Emission Detection," *Sensors and Actuators: A Physical*, Vol.99, No.3, 2002, pp.236-243.
7. Breckenridge, F.R., M. Greenspan, "Surface-wave Displacement: Absolute Measurements Using a Capacitive Transducer," *Journal of Acoustic Society of America*, Vol.69, April 1981, pp.1177-1185.
8. Khuri-Yakub, B.T., F.L. Degertekin, X-C. Jin, S. Calmes, I. Ladabaum, S. Hansen, X.J. Zhang, "Silicon Micromachined Ultrasonic Transducers," *1998 IEEE Ultrasonics Symposium*, pp.985-991.
9. Jin, X-C., I. Ladabaum, B.T. Khuri-Yakub, "The Microfabrication of Capacitive Ultrasonic Transducers," *Journal of Micromechanical Systems*, Vol.7, No.3, Sep. 1998, pp.295-302.
10. Jin, X-C., I. Ladabaum, F.L. Degertkin, S. Calmes, B.T. Khuri-Yakub, "Fabrication and Characterization of Surface Micromachined Capacitive Ultrasonic Immersion Transducers," *IEEE Journal of Micromechanical Systems*, Vol.8, No.1, Mar. 1999, pp.100-114.
11. Bashford, A.G., D.W. Schindel, D.A. Hutchins, "Micromachined Ultrasonic Capacitance Transducers for Immersion Applications," *IEEE Transactions on Ultrasonics, Ferroelectrics, and Frequency Control*, Vol.45, No.2, Mar. 1998, pp.367-375.
12. Greve, D., I. Oppenheim, A. Jain, "Electrical characterization of coupled and uncoupled MEMS ultrasonic transducers," *IEEE Transactions on Ultrasonics, Ferroelectrics, and Frequency Control*, accepted for publication.
13. Jain, A., "In Situ Ultrasonic MEMS Transducer for Detecting Flaws in Structural Materials," M.S. Thesis, Carnegie Mellon University, 2002.
14. Scheibner, D., J. Wibbeler, and J. Mehner, "Frequency Selective Sensor Arrays for Vibration Measurement," *IEEE Sensors 2002*, June, 2002.
15. Yan, T., P.Theobald, B.E.Jones, "Self-calibrating Piezoelectric Transducer with Integral Sensor for In Situ Energy Calibration of Acoustic Emission," *NDT&E International*, Vol.35, 2002, pp.459-464.
16. Liew, K.M., C.M.Wang, Y.Xiang, S.Kitipornchai, *Vibration of Plates*, Elsevier, 1998.